Order online now!

www.rockland.com
tech@rockland.com
+1 484.791.3823

Datasheet for 610-1302

Mouse IgG (H&L) Antibody Peroxidase Conjugated

Overview

Description:	Goat Anti-Mouse IgG (H&L) Antibody Peroxidase Conjugated - 610-1302
Item No.:	610-1302
Size:	2 mg
Applications:	ELISA, WB, IF, IHC, Other
Reactivity:	Mouse
Host Species:	Goat

Product Details

Background:	Secondary antibodies bind to the primary antibody to assist in detection, sorting and purification of target antigens. To enable detection, the secondary antibody must have specificity for the antibody species and isotype of the primary antibody being used and generally is conjugated. Rockland produces highly active antibodies and conjugates against mouse immunoglobulins. Anti-Mouse Secondary Antibodies are affinity-purified polyclonal antibodies with well-characterized specificity for mouse immunoglobulin classes, subclasses, and fragments. They are available as unlabeled antibodies as well as conjugates of alkaline phosphatase (AP), horseradish peroxidase (HRP), fluorescent conjugates, and biotin. This Anti-MOUSE IgG generated in goat is designed to detect heavy and light chains (H&L) and has been Peroxidase (HRP) conjugated. Rigorous quality control testing ensures that the finished product meets or exceeds out high standards for optimum performance in your assays. These secondary antibodies are used throughout various types of assays, including ELISA or Western Blot, Immunohistochemistry, Flow Cytometry. Optimal secondary antibody requires knowledge of the detection assay.
Synonyms:	Goat Anti-Mouse IgG Secondary Antibody Peroxidase Conjugated, Goat Anti-Mouse IgG Secondary Antibody HRP Conjugated, GAM-HRP, Anti-mouse secondary antibody, anti-mouse HRP antibody, horseradish peroxidase conjugated secondary antibody, anti-mouse horseradish peroxidase conjugated secondary antibody
Host Species:	Goat
Specificity:	IgG (H&L)
Conjugate:	Peroxidase (HRP)
Clonality:	Polyclonal

Format:	IgG
F/P Ratio:	0.43

Target Details

Reactivity:	Mouse
Immunogen Type:	Native Protein
Immunogen:	Anti-Mouse IgG whole molecule was produced by repeated immunization with Mouse IgG whole molecule in goat.
Purity/Specificity:	MOUSE IgG (H&L) Antibody Peroxidase Conjugated was prepared from monospecific antiserum by immunoaffinity chromatography using Mouse IgG coupled to agarose beads followed by solid phase adsorption(s) to remove any unwanted reactivities. Assay by immunoelectrophoresis resulted in a single precipitin arc against anti-Peroxidase, anti-Goat Serum, Mouse IgG and Mouse Serum.
Relevant Links:	• 610-1302 SDS

Application Details

Tested Applications:	ELISA, WB
Suggested Applications:	IF, IHC, Other (Based on references)
Application Note:	Anti-Mouse secondary antibody conjugated to horseradish peroxidase (HRP) generated in goat detects specifically Mouse IgG whole molecule. This anti-Mouse HRP antibody has been tested by ELISA and western blot and is suitable for ELISA, Sandwich ELISA, titration assays, western-blot, immunoprecipitation, Immunohistochemistry as well as other HRP antibody based assays. Specific conditions for reactivity and signal detection should be optimized by the end user.
Assay Dilutions:	All assays should be optimized by the user. Recommended dilutions (if any) may be listed below.
ELISA:	1:1,000 - 1:20,000
IHC:	1:500 - 1:2,500
WB:	1:2,000 - 1:10,000

Formulation

Physical State:	Lyophilized
Concentration:	2 mg/mL by UV absorbance at 280 nm

Buffer:	0.02 M Potassium Phosphate, 0.15 M Sodium Chloride, pH 7.2
Preservative:	0.01% (w/v) Gentamicin Sulfate. Do NOT add Sodium Azide!
Stabilizer:	10 mg/mL Bovine Serum Albumin (BSA) - Immunoglobulin and Protease free
Reconstitution Volume:	1.0 mL
Reconstitution Buffer:	Restore with deionized water (or equivalent)

Shipping & Handling

Shipping Condition:	Ambient
Storage Condition:	Store HRP Conjugated Mouse Secondary Antibody at 4° C prior to restoration. For extended storage aliquot contents and freeze at -20° C or below. Avoid cycles of freezing and thawing. Centrifuge product if not completely clear after standing at room temperature. This product is stable for several weeks at 4° C as an undiluted liquid. Dilute only prior to immediate use.
Expiration:	Expiration date is one (1) year from date of receipt.

Images

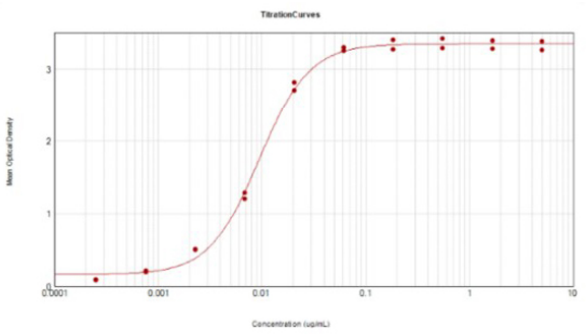

ELISA
ELISA Results of Goat Anti-Mouse IgG Peroxidase Conjugated Antibody tested against purified Mouse IgG protein. Each well was coated in duplicate with 10 µg of Mouse IgG (p/n 010-0102). The starting dilution of antibody was 5µg/ml and the X-axis represents the Log10 of a 3-fold dilution. The titer is 1:106,000. This titration is a 4-parameter curve fit where the IC50 is defined as the titer of the antibody. Assay performed using 3% fish gelatin as blocking buffer and TMB substrate p/n TMBE-1000.

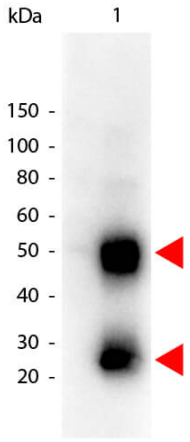

Western Blot
Western Blot of Peroxidase conjugated Goat anti-Mouse IgG antibody. Lane 1: Mouse IgG. Lane 2: none. Load: 50 ng per lane. Primary antibody: none. Secondary antibody: Peroxidase goat secondary antibody at 1:1,000 for 60 min at RT. Block: MB-070 30 min at RT. Predicted/Observed size: 50 kDa, 25 kDa for Mouse IgG. Other band(s): none.

References

- Steding H et al. Lentiviral rescue of UMPS auxotrophy enables drug-free selection and stable vector expression. *Mol Ther Adv.* (2026)
- Lopez-Garcia OK et al. Coupling Far-Western Blotting with Peptide Microarrays Reveals Novel E-Cadherin Spore-Surface Ligands in Clostridioides difficile. *J Proteome Res.* (2026)
- Koch C et al. Analysis of 173,303 exomes and genomes in the Pakistan Genome Resource. *Nature.* (2026)
- Ugalde V et al. Preclinical evaluation of nitrated α-synuclein-specific CAR-Treg therapy in Parkinson's disease. *Cell Rep Med.* (2026)
- Swaroop B SS et al. PAK1 mediated phosphorylation of ARGLU1 promotes tumorigenic potential of Breast cancer. *J Biol Chem.* (2026)
- Ramos B et al. MAVS oligomerization drives a faster and more efficient antiviral signaling activation at peroxisomes compared to mitochondria. *FEBS J.* (2026)
- Mukinovic E et al. Overcoming acquired doxorubicin resistance of ovarian carcinoma cells by verapamil-mediated promotion of DNA damage-driven cytotoxicity. *Int J Oncol.* (2026)
- Karakus E et al. Novel SOAT inhibitors block DHEAS transport and suppress proliferation in MCF-7 breast cancer cells. *Sci Rep.* (2026)
- Chia JC et al. CITF1 interacts with FIT and regulates copper-iron crosstalk in Arabidopsis. *Plant Cell.* (2026)
- Lloyd HC et al. A method for the detection and enrichment of endogenous cereblon substrates. *Cell Chem Biol.* (2026)
- Cai Y et al. Circular RNA circHomer1 mediates hippocampal functions via ribonucleoprotein granule transport and dendritic targeting of synaptic RNAs. *Sci Adv.* (2026)
- Lin Z et al. Temporal photoproximity labeling of ligand-activated EGFR neighborhoods using MultiMap. *Nat Chem Biol.* (2026)

- Diehl A et al. Conservation and Specificity in Bacillus Biofilm Dynamics: On Structure and Function of B. cereus Camelysins. *JMB.* (2026)
- Kusumawati S et al. Thymoquinone and madecassoside improve motor function in a rotenone-induced mouse model of early Parkinson's disease: Role of dopamine, alpha-synuclein and mBDNF. *Narra J.* (2025)
- Laine C et al. Characterization of the Regulatory AAA-ATPase Subunit Rpt3 in Plasmodium berghei as an Activator of Protein Phosphatase 1. *Int J Mol Sci.* (2025)
- Liu Z et al. Sterol-C4-methyl-oxidase Erg251 governs Candida albicans hypoxic growth, commensalism and virulence. *Nat Commun.* (2025)
- Murugan S et al. Pak1 dysregulates pyruvate metabolism in PDAC cells by exerting a phosphorylation-mediated regulatory effect on PDHA1. *J Biol Chem.* (2025)
- Mohsen JJ et al. Cellular function of the GndA microprotein during heat shock. *bioRxiv [Preprint].* (2025)
- Hines MA et al. Elp1 function in placode-derived neurons is critical for proper trigeminal ganglion development. *Dev Dyn.* (2025)
- Abbad A et al. Co-administration of seasonal quadrivalent influenza and COVID-19 vaccines leads to enhanced immune responses to influenza virus and reduced immune responses to SARS-CoV-2 in naive mice. *Vaccine.* (2025)
- Huilcaman R et al. Inclusion of AVβ3 integrin into extracellular vesicles in a caveolin-1 tyrosine-14- phosphorylation dependent manner and subsequent transfer to recipient melanoma cells promotes migration, invasion and metastasis. *Cell Commun Signal.* (2025)
- Tursi NJ et al. Modulation of lipid nanoparticle-formulated plasmid DNA drives innate immune activation promoting adaptive immunity. *Cell Rep Med.* (2025)
- Perez-Moreno E et al. Endogenous Galectin-8 protects against Th17 infiltration and fibrosis following acute kidney injury. *Mol Med.* (2025)
- Singh G et al. Characterization of the glycoproteins of fish and amphibian influenza B-like viruses. *Sci Adv.* (2025)
- Papadopoulos E et al. Therapeutic doses of methylphenidate following repetitive mild traumatic brain injury transiently disrupts risk/reward decision making in a sex dependent manner. *Exp Neurol.* (2025)
- Bai S et al. A Novel Cranial Bone Transport Technique Repairs Skull Defect and Minimizes Brain Injury Outcome in Traumatic Brain Injury Rats. *Adv Sci (Weinh).* (2025)
- Alabi Y et al. Lamin B1 and LAP2β resist cytoskeletal force to maintain lamin A/C meshwork organization and preserve nuclear integrity. *Mol Biol Cell.* (2025)
- Marin HC et al. The nuclear periphery confers repression on H3K9me2-marked genes and transposons to shape cell fate. *Nat Cell Biol.* (2025)
- Jayatissa A et al. The ERVK3-1 Microprotein Interacts with the HUSH Complex. *Biochemistry.* (2025)
- Nishimura S et al. HSC70 coordinates COP9 signalosome and SCF ubiquitin ligase activity to enable a prompt stress response. *EMBO Rep.* (2025)
- Wu CY et al. Luteinizing Hormone Induces Murine Hair Loss through Transient Receptor Potential Canonical Channel-Mediated Cell Aging Responses: Implications for Female Pattern Hair Loss Pathogenesis. *J Invest Dermatol.* (2025)
- Ramirez-Velez I et al. Paracellular Delivery of Protein Drugs with Smart EnteroPatho Nanoparticles. *ACS Nano.* (2024)

- Kücük P et al. Cardiomyocytes, cardiac endothelial cells and fibroblasts contribute to anthracycline-induced cardiac injury through RAS-homologous small GTPases RAC1 and CDC42. *Pharmacol Res.* (2024)
- Kim Y et al. β-carotene attenuates muscle wasting in cancer cachexia by regulating myogenesis and muscle atrophy. *Oncol Rep.* (2024)
- Cruz P et al. Unraveling the Role of JMJD1B in Genome Stability and the Malignancy of Melanomas. *Int J Mol Sci.* (2024)
- Sun Y et al. Methionine availability influences essential H3K36me3 dynamics during cell differentiation. *bioRxiv [Preprint].* (2023)
- Montero DA et al. A chimeric protein-based vaccine elicits a strong IgG antibody response and confers partial protection against Shiga toxin-producing Escherichia coli in mice. *Front Immunol.* (2023)
- Castro-Córdova P et al. Redistribution of the Novel Clostridioides difficile Spore Adherence Receptor E-Cadherin by TcdA and TcdB Increases Spore Binding to Adherens Junctions. *Infect Immun.* (2023)
- Liu M et al. Co-culture models of endothelial cells, macrophages, and vascular smooth muscle cells for the study of the natural history of atherosclerosis. *PLoS One.* (2023)
- Bina P et al. Neurogenin 2 and Neuronal Differentiation 1 Control Proper Development of the Chick Trigeminal Ganglion and Its Nerve Branches. *J Dev Biol.* (2023)
- Hummels KR et al. Coordination of bacterial cell wall and outer membrane biosynthesis. *Nature.* (2023)
- Thakkar A et al. Study of efficacy and longevity of immune response to third and fourth doses of COVID-19 vaccines in patients with cancer: A single arm clinical trial. *Elife.* (2023)
- Haimi CA et al. Neural crest cell-placodal neuron interactions are mediated by Cadherin-7 and N-cadherin during early chick trigeminal ganglion assembly. *F1000Res.* (2022)
- Hormazabal J et al. Chaperone mediated autophagy contributes to the newly synthesized histones H3 and H4 quality control. *Nucleic Acids Res.* (2022)
- Strohmeier, S et al. A CpG 1018 adjuvanted neuraminidase vaccine provides robust protection from influenza virus challenge in mice. *Npj Vaccines* (2022)
- Carreno JM et al. Evidence for retained spike-binding and neutralizing activity against emerging SARS-CoV-2 variants in serum of COVID-19 mRNA vaccine recipients. *EBioMedicine* (2021)
- Arunkumar GA et al. Functionality of the putative surface glycoproteins of the Wuhan spiny eel influenza virus. *Nat Commun.* (2021)
- Ortega L et al. The Ω-3 fatty acid docosahexaenoic acid selectively induces apoptosis in tumor-derived cells and suppress tumor growth in gastric cancer. *Eur J Pharmacol.* (2021)
- Ortega L et al. The Ω-3 fatty acid docosahexaenoic acid selectively induces apoptosis in tumor-derived cells and suppress tumor growth in gastric cancer. *Eur J Pharmacol.* (2021)
- Yang X, He Z, Zhang G, et al. Evaluation of Reactivity of Monoclonal Antibodies Against Omp25 of Brucella spp. *Front Cell Infect Microbiol.* (2020)
- Amanat F, Stadlbauer D, Strohmeier S, et al. A serological assay to detect SARS-CoV-2 seroconversion in humans. *Nat. Med.* (2020)

- Ramirez DH, Aonbangkhen C, Wu HY, et al. Engineering a Proximity-Directed O-GlcNAc Transferase for Selective Protein O-GlcNAcylation in Cells. *ACS Chem Biol.* (2020)
- Fegan, JE et al. Utility of Hybrid Transferrin Binding Protein Antigens for Protection Against Pathogenic Neisseria Species. *Frontiers in Immunology* (2019)
- Gerber KJ, Squires KE, Hepler JR. 14-3-3γ binds regulator of G protein signaling 14 (RGS14) at distinct sites to inhibit the RGS14:Gαi-AlF4- signaling complex and RGS14 nuclear localization. *J Biol Chem.* (2019)
- Jiang S, Xu Y. Annexin A2 upregulation protects human retinal endothelial cells from oxygen-glucose deprivation injury by activating autophagy. *Exp Ther Med.* (2019)
- Noppes S, Müller SF, Bennien J, et al. Homo- and heterodimerization is a common feature of the solute carrier family SLC10 members. *Biol Chem.* (2019)
- Wang XX, Zhang H, Li Y. Preliminary study on the role of miR148a and DNMT1 in the pathogenesis of acute myeloid leukemia. *Mol Med Rep.* (2019)
- Henninger C, Pohlmann S, Ziegler V, Ohlig J, Schmitt J, Fritz G. Distinct contribution of Rac1 expression in cardiomyocytes to anthracycline-induced cardiac injury. *Biochem Pharmacol.* (2019)
- Sanderson SM, Mikhael PG, Ramesh V, Dai Z, Locasale JW. Nutrient availability shapes methionine metabolism in p16/MTAP-deleted cells. *Sci Adv.* (2019)
- Lin N, Dong XJ, Wang TY, et al. Characteristics of olfactory ensheathing cells and microarray analysis in Tupaia belangeri (Wagner, 1841). *Mol Med Rep.* (2019)
- Gallardo et al. Effect of Breed on Transcriptional and Protein Expression of Lipogenic Enzymes in Tail and Subcutaneous Adipose Tissue from Two Grazing Breeds of Lambs. *Animals* (2019)
- Elsaeidi et al. Notch Suppression Collaborates with Ascl1 and Lin28 to Unleash a Regenerative Response in Fish Retina, But Not in Mice. *The Journal of Neuroscience* (2018)
- Spasojevic et al. PKD1 is a potential biomarker and therapeutic target in triple-negative breast cancer. *Oncotarget* (2018)
- Ray et al. Regulation of Trypanosoma brucei Acetyl Coenzyme A Carboxylase by Environmental Lipids. *mSphere* (2018)
- Rahman MT, Ghosh C, Hossain M, et al. IFN-γ, IL-17A, or zonulin rapidly increase the permeability of the blood-brain and small intestinal epithelial barriers: Relevance for neuro-inflammatory diseases. *Biochem Biophys Res Commun.* (2018)
- Liberti et al. A Predictive Model for Selective Targeting of the Warburg Effect through GAPDH Inhibition with a Natural Product. *Cell Metabolism* (2017)
- Ciesielska A et al. Bis (monoacylglycero) phosphate inhibits TLR4-dependent RANTES production in macrophages. *Int J Biochem Cell Biol.* (2017)
- Emanuela Piermarini et al. Frataxin silencing alters microtubule stability in motor neurons: implications for Friedreich's ataxia. *Hum Mol Genet.* (2016)
- Neiser et al. Assessment of Dextran Antigenicity of Intravenous Iron Preparations with Enzyme-Linked Immunosorbent Assay (ELISA). *International Journal of Molecular Sciences* (2016)
- Mendez et al. Endoplasmic reticulum stress-independent activation of unfolded protein response kinases by a small molecule ATP-mimic. *Elife* (2015)

- Turner, NA et al. Factor VIII Is Synthesized in Human Endothelial Cells, Packaged in Weibel-Palade Bodies and Secreted Bound to ULVWF Strings. *PloS One* (2015)
- Ohta H, Sunden Y, Yokoyama N, et al. Expression of apical junction complex proteins in duodenal mucosa of dogs with inflammatory bowel disease. *Am J Vet Res.* (2014)
- Xu S, Grande F, Garofalo A, Neamati N. Discovery of a novel orally active small-molecule gp130 inhibitor for the treatment of ovarian cancer. *Mol Cancer Ther.* (2013)
- Junk DJ, Cipriano R, Stampfer M, Jackson MW. Constitutive CCND1/CDK2 activity substitutes for p53 loss, or MYC or oncogenic RAS expression in the transformation of human mammary epithelial cells. *PLoS One.* (2013)
- Pullen NA, Anand M, Cooper PS, Fillmore HL. Matrix metalloproteinase-1 expression enhances tumorigenicity as well as tumor-related angiogenesis and is inversely associated with TIMP-4 expression in a model of glioblastoma. *J Neurooncol.* (2012)
- Horn P et al. Circulating microparticles carry a functional endothelial nitric oxide synthase that is decreased in patients with endothelial dysfunction. *J Am Heart Assoc.* (2012)
- Zong M, Satoh A, Yu MK, et al. TRAPPC9 mediates the interaction between p150 and COPII vesicles at the target membrane. *PLoS One.* (2012)
- Den Herder G, Yoshida S, Antolín-Llovera M, Ried MK, Parniske M. Lotus japonicus E3 ligase SEVEN IN ABSENTIA4 destabilizes the symbiosis receptor-like kinase SYMRK and negatively regulates rhizobial infection. *Plant Cell.* (2012)
- LeVine H et al. Dihydroxybenzoic acid isomers differentially dissociate soluble biotinyl-Aβ(1-42) oligomers. *Biochemistry* (2012)
- Zhang X et al. Vaccination with different M2e epitope densities confers partial protection against H5N1 influenza A virus challenge in chickens. *Intervirology.* (2011)
- Ohta H, Yamaguchi T, Rajapakshage BK, et al. Expression and subcellular localization of apical junction proteins in canine duodenal and colonic mucosa. *Am J Vet Res.* (2011)
- McCall LI et al. Localization and induction of the A2 virulence factor in Leishmania: evidence that A2 is a stress response protein. *Mol Microbiol.* (2010)
- Reeves TM et al. Proteolysis of submembrane cytoskeletal proteins ankyrin-G and αII-spectrin following diffuse brain injury: a role in white matter vulnerability at Nodes of Ranvier. *Brain Pathology (Zurich, Switzerland)* (2010)
- Pullen NA, Fillmore HL. Induction of matrix metalloproteinase-1 and glioma cell motility by nitric oxide. *J Neurooncol.* (2010)
- Mafra D, Santos FR, Lobo JC, et al. Alpha-tocopherol supplementation decreases electronegative low-density lipoprotein concentration [LDL(-)] in haemodialysis patients. *Nephrol Dial Transplant.* (2009)
- Lobo J, Santos F, Grosso D, et al. Electronegative LDL and lipid abnormalities in patients undergoing hemodialysis and peritoneal dialysis. *Nephron Clin Pract.* (2008)
- Oliveira JA, Sevanian A, Rodrigues RJ, Apolinário E, Abdalla DS. Minimally modified electronegative LDL and its autoantibodies in acute and chronic coronary syndromes. *Clin Biochem.* (2006)
- Dennison AC, Van Metre DC, Morley PS, Callan RJ, Plampin EC, Ellis RP. Comparison of the odds of isolation, genotypes, and in vivo production of major toxins by Clostridium perfringens obtained from the gastrointestinal tract of dairy cows with hemorrhagic bowel syndrome or left-displaced abomasum. *J Am Vet Med Assoc.* (2005)

- Van Komen JS et al. The polybasic juxtamembrane region of Sso1p is required for SNARE function in vivo. *Eukaryot Cell.* (2005)

Disclaimer

This product is for research use only and is not intended for therapeutic or diagnostic applications. Please contact a technical service representative for more information. All products of animal origin manufactured by Rockland Immunochemicals are derived from starting materials of North American origin. Collection was performed in United States Department of Agriculture (USDA) inspected facilities and all materials have been inspected and certified to be free of disease and suitable for exportation. All properties listed are typical characteristics and are not specifications. All suggestions and data are offered in good faith but without guarantee as conditions and methods of use of our products are beyond our control. All claims must be made within 30 days following the date of delivery. The prospective user must determine the suitability of our materials before adopting them on a commercial scale. Suggested uses of our products are not recommendations to use our products in violation of any patent or as a license under any patent of Rockland Immunochemicals, Inc. If you require a commercial license to use this material and do not have one, then return this material, unopened to: Rockland Inc., P.O. BOX 5199, Limerick, Pennsylvania, USA.